Reports

Uplifted Trench Sediments: Southwestern Alaska–Bering Shelf Edge

Abstract. *Cretaceous turbidites are discontinuously exposed for 1700 kilometers along the continental margin of southwestern Alaska and the Bering shelf edge. Paleocurrent flow parallel to exposure patterns and the abundance of primary andesitic volcanic detritus suggest deposition in an oceanic trench. This Cretaceous trench bordering the continent was superseded by the Aleutian arc-trench in the earliest Tertiary.*

Movements of ancient crustal plates are recorded on the deep-sea floor by patterns of magnetic anomalies (*1*), trends of fracture zones (*2*), and elongation of aseismic ridges (*3*). Paleomagnetic and geologic data from the continents also provide indications of previous plate motions. Recent work (*4*) suggests that oceanic crust is consumed along deep-sea trenches, with the result that magnetic anomalies, fracture zones, and aseismic ridges are destroyed. Thus, paleomagnetic data and ancient plate boundaries, conserved on continents, assume increasing importance in Mesozoic and Paleozoic plate-tectonic reconstructions. Specifically, various interpretations (*5, 6, 7*) of Mesozoic paleogeography and plate geometry in the northernmost Pacific Ocean–Bering Sea region depend partially on whether the boundary between the ocean and the continent is interpreted as a trench or as a continental slope and rise. New data on primary sedimentary structures and the composition of Cretaceous turbidites exposed along the southwestern coast of Alaska suggest that they were deposited in a trench. These rocks have been subsequently folded, uplifted, and accreted onto the continental margin. The formation of the Aleutian arc-trench during the latest Cretaceous or earliest Tertiary (*8*) separated the Bering Sea from the Pacific Ocean, cut across the Cretaceous structures at the southwestern end of the Alaskan continental margin, and marked a significant shift in a crustal plate boundary.

A deepwater sedimentary and igneous sequence of Triassic to Eocene age forms the backbone of the Shumagin-Kodiak shelf southeast of the Alaska Peninsula. This sequence includes bedded cherts, ultramafic rocks, basic volcanics, and a thick series of complexly folded, interbedded sandstones and mudstones. Burk (*7*) and Scholl *et al.* (*5*) correlate these rocks with a late Mesozoic sedimentary and volcanic sequence in the Koryak Mountains of eastern Siberia and suggest that the Bering shelf edge was a connecting link. The existence of this connection is supported by samples of Cretaceous turbidites from the acoustic basement of the Bering shelf edge in the Pribilof submarine canyon [Fig. 1; (*9*)]. Furthermore, structural trends within the Cretaceous rocks along the Shumagin-Kodiak shelf and Bering shelf edge (*10*) are parallel to exposure patterns, which implies original continuity.

Cretaceous deepwater sedimentary rocks compose most of the exposed rock along the Shumagin-Kodiak shelf. Older sedimentary rocks, where exposed, are located landward of the Cretaceous sandstones and mudstones, whereas younger rocks are found seaward (*10*). Thus, the apparent loci of deposition decrease in age from continent to ocean within the Triassic to Eocene deepwater sediments.

The Cretaceous sedimentary rocks have been studied intensively near the junction of the Shumagin-Kodiak shelf and the Bering shelf edge (*10*). Here, in the Shumagin and Sanak islands (Fig. 1), the sequence is composed of monotonous sections of thin (4 cm) to thick (10 m) bedded sandstones and mudstones. These rocks show grading, convolute lamination, and groove and flute casts. They were apparently deposits by turbidity currents. The turbidites include trace fossils (for example, *Helminthoida crassa*) similar to feeding tracks observed on the modern deep-sea floor (*11*) but contain no shallow-water shelly fauna. These factors suggest deepwater accumulation.

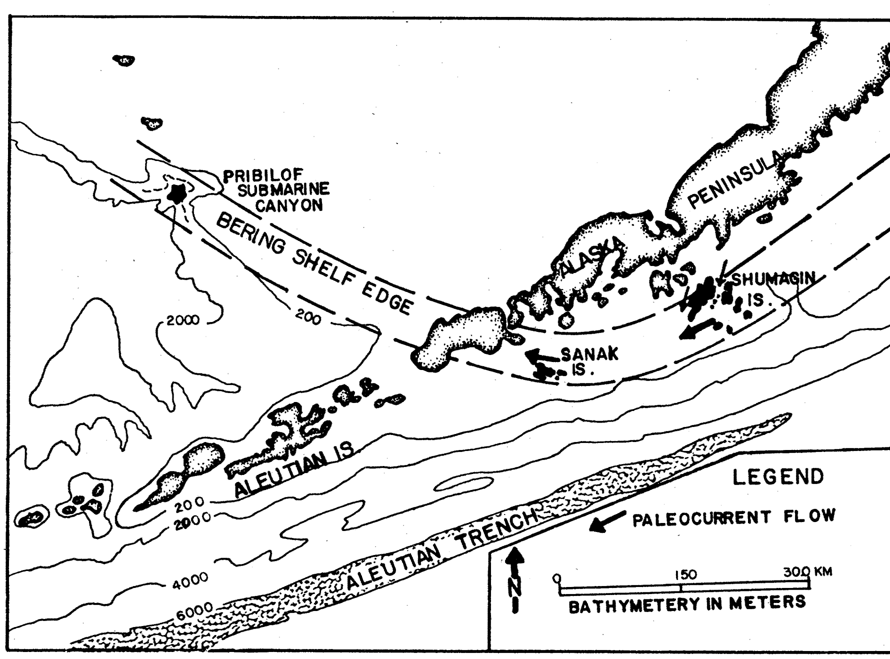

Fig. 1. Outcrop patterns of Cretaceous turbidites shown in black include dredged basement exposure in the Pribilof submarine canyon. The arrows indicate the directions of flow of Cretaceous turbidity currents.

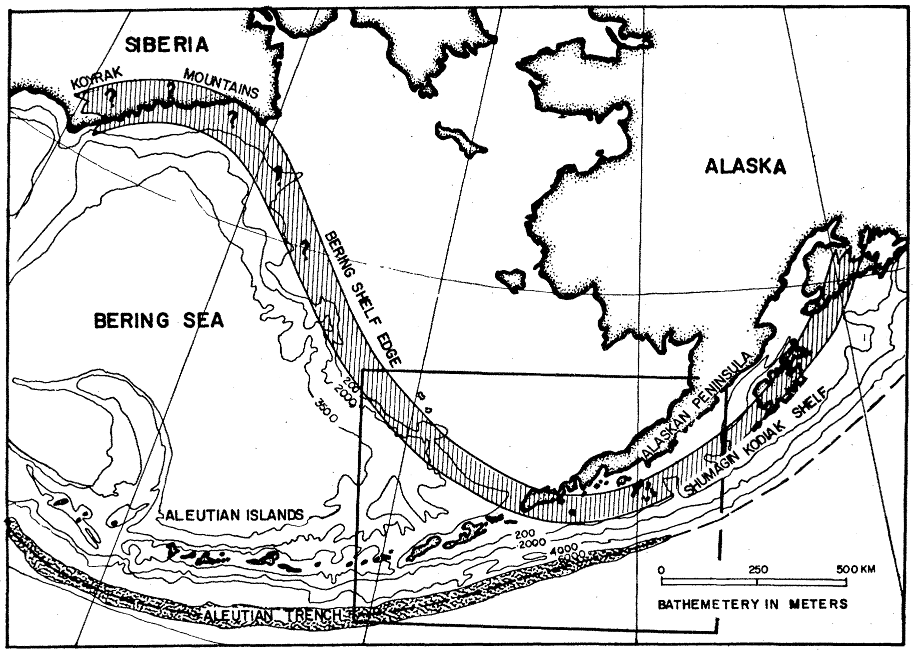

Fig. 2. Vertical lined pattern indicates the probable location of the Cretaceous trench, inferred from the exposure pattern of Cretaceous deepwater sediments.

Microscopic analyses of 61 sandstones show that their average composition is 14 percent quartzose grains, 28 percent feldspar, 48 percent rock fragments, and 10 percent matrix. Andesitic volcanic detritus accounts for 96 percent of the rock fragments. Devitrified glass shards, long-tube pumice, and local ash beds suggest a primary source for the abundant volcanic material.

Large numbers of basal current markings indicate the directions of Cretaceous turbidite flow. In the Sanak Islands, 157 groove casts and 29 flute casts (*12*) specify paleocurrent flow to the west-northwest (grand mean 292°, standard deviation ± 30°). Thus, ancient current flow trended from the tip of the Alaska Peninsula parallel to the Bering shelf edge. In the Shumagin Islands, 287 groove casts and 108 flute casts indicate paleocurrent movement to the southwest (grand mean 212°, standard deviation ± 42°). Locally bimodal current directions suggest that the Shumagin grand mean is composed of a major component directed west-southwest (239°), with subsidiary flow to the south-southwest [199°; (*10*)]. In the Shumagin Islands, turbidity currents originating from the north apparently veered to the west-southwest, trending toward the Sanak Islands. In general, paleocurrent flow parallels the edge of the present continental shelf and Cretaceous turbidite outcrop patterns; current directions vary from an orientation along the Shumagin-Kodiak shelf to a direction parallel to the Bering shelf edge (Fig. 1). These relations suggest sedimentary continuity from the Cretaceous turbidites of the Shumagin-Kodiak shelf to the acoustic basement of the Bering shelf edge.

Basin slope is assumed to have been the primary factor controlling the flow of turbidity currents. Medium grain size, graded bedding, and sole marks distinguish the Cretaceous turbidites from interbedded muds and thin silt layers deposited by contour currents along the continental rise of eastern North America (*13*). Moreover, recent work (*14*) suggests that major gravity-induced sediment transport across the continental rise is unaffected by the geostrophic currents. The paleocurrent data of this report are interpreted as the result of gravity flow in the depositional framework of modern continental margins. Possible environments of accumulation include a deep-sea fan or continental rise, a borderland basin or marginal ocean basin (*15*), or a trench.

Transport by turbidity currents across deep-sea fans and continental rises is inconsistent with the predominantly longitudinal paleocurrent flow of the Cretaceous turbidites of southwestern Alaska. A borderland basin or marginal ocean basin following the trend of the Cretaceous exposures could account for the observed current directions of lateral feed and longitudinal flow. However, borderland basins and marginal ocean basins must be enclosed on the seaward side by an uplifted basement terrain older than the accumulated sediments. No rocks older than the Cretaceous sediment are found on their seaward side along the Kodiak, Shumagin, or Bering shelf edges. A trough at the edge of the continental margin, a trench, is the most likely depositional site of the Cretaceous turbidites. A trench permits the axial confinement of any lateral turbidity flow, as demanded by the paleocurrent data. The oceanic crust enclosing the seaward side of the trench was presumably subducted during underthrusting. Recent trenches are almost always bordered on the landward side by composite volcanoes. Thus, trench deposition of the Cretaceous turbidites is consistent with their abundance of primary volcanic detritus. Recent trenches show longitudinal submarine channels (*16*), presumably due to axial current flow.

The parallelism of outcrop patterns and dominant current directions (Fig. 1) suggests extension of the trench interpretation through the Cretaceous turbidite exposures bordering the southern and western margin of the Alaska subcontinent (Fig. 2). Along the Shumagin-Kodiak shelf the trench deposits were complexly deformed with fold axes trending parallel to the present shelf edge and axial surfaces overturned seaward (*10*). They were uplifted and intruded by granodioritic and quartz-dioritic plutons dated at 56 to 64 million years ago (*7*, *10*).

The Aleutian arc-trench system was probably initiated in the latest Cretaceous or earliest Tertiary (*8*); it now extends seaward (south) of the postulated Cretaceous trench. To the west, the proposed location of the Cretaceous trench is now separated from the Aleutian trench by the Bering Sea (Fig. 2). Since the Bering Sea contains sediments at least as old as early Tertiary (*5*), it must have been defined, by whatever process, during the transition between the Cretaceous and Aleutian trenches. Along the Shumagin-Kodiak shelf, the trench transition involved a seaward migration of 100 to 200 km (Fig. 2). This transition is consistent with tectonic histories of this region proposed by Burk (*7*) and Scholl *et al.* (*5*) on more fragmentary evidence. The development of the Aleutian arc-trench and the consequent shift in a crustal plate boundary closely preceded or coincided with early Tertiary uplift and intrusion of the Cretaceous trench deposits.

J. CASEY MOORE
Earth Sciences, University of California, Santa Cruz 95060

References and Notes

1. F. J. Vine, *Science* **154**, 1405 (1966).
2. W. J. Morgan, *J. Geophys. Res.* **73**, 1959 (1968); X. LePichon, *ibid.*, p. 3661.
3. W. J. Morgan, *Nature* **230**, 42 (1971).
4. B. Isacks, J. Oliver, L. R. Sykes, *J. Geophys. Res.* **73**, 5855 (1968).
5. D. W. Scholl, E. C. Buffington, M. S. Marlow, *Geol. Soc. Amer. Spec. Pap.*, in press.
6. J. G. Jones, *Nature* **229**, 400 (1971); W. C. Pitman, III, and D. E. Hayes, *J. Geophys. Res.* **73**, 6571 (1968).
7. C. A. Burk, *Geol. Soc. Amer. Mem. 99* (1965).
8. D. W. Scholl, H. G. Greene, M. S. Marlow, *Geol. Soc. Amer. Bull.* **81**, 3583 (1970).
9. D. M. Hopkins, D. W. Scholl, W. O. Addicott, R. L. Pierce, P. B. Smith, J. A. Wolfe, D. Gershanovich, B. Kotenev, K. E. Lohman, J. H. Lipps, J. Obradovich, *ibid.* **80**, 1471 (1969).
10. J. C. Moore, thesis, Princeton University (1971).
11. A. Seilacher, *Mar. Geol.* **5**, 413 (1967).
12. Flute casts provide an absolute sense of turbidity-current flow; groove casts give only a linear reading. Flute casts are used locally to interpret the actual flow directions of groove casts.
13. B. C. Heezen, C. D. Hollister, W. F. Ruddiman, *Science* **152**, 502 (1966).
14. D. J. Stanley, H. Sheng, C. P. Pedraza, *Geol. Soc. Amer. Bull.* **87**, 1831 (1971).
15. D. Karig, *J. Geophys. Res.* **76**, 2592 (1971).
16. R. von Huene and G. G. Shor, Jr., *Geol. Soc. Amer. Bull.* **80**, 1889 (1969); D. W. Scholl, M. N. Christensen, R. von Huene, M. S. Marlow, *ibid.* **81**, 1339 (1970).
17. Supported by the Mobil Oil Corporation, the Atlantic Richfield Company, the Department of Geological and Geophysical Sciences and the Boyd Fund of Princeton University, and the U.S. Geological Survey. I thank C. A. Burk and F. B. Van Houten for assistance in all phases of this work; D. W. Scholl, E. C. Buffington, and M. S. Marlow for a preprint of their paper (5); and R. E. Garrison and R. von Huene for criticism of the final manuscript. This report is based on a thesis submitted to Princeton University in partial fulfillment of the requirements for the Ph.D. degree.

6 December 1971; revised 19 January 1972

3C279: Evidence for a Non-Superrelativistic Model

Abstract. *Measurements of the variation of the total flux density of the quasi-stellar radio source 3C279 provide evidence for an alternate model to explain the recently reported apparent source expansion rate of ten times the speed of light.*

In a recent report, Knight *et al.* (*1*) presented some very-long-baseline interferometry (VLBI) observations which showed that the quasi-stellar source 3C279 had a complex angular structure on a scale of 10^{-3} arc second. In a subsequent report by the same group, Whitney *et al.* (*2*) showed that the null of the interferometric fringe amplitude function was displaced from the position they had observed 4 months earlier. The above authors interpreted their observed fringe amplitude curves as having been produced by two nearly point sources, which must be of nearly equal flux density, since a deep null exists in the fringe amplitude curve. In terms of this model the observed displacement of the null was interpreted as being the result of an increase in the angular separation of the two components which, when converted to a velocity of separation (with the assumption of a cosmological distance for 3C279), gave an apparent speed of 10 ± 3 times the speed of light (*3*).

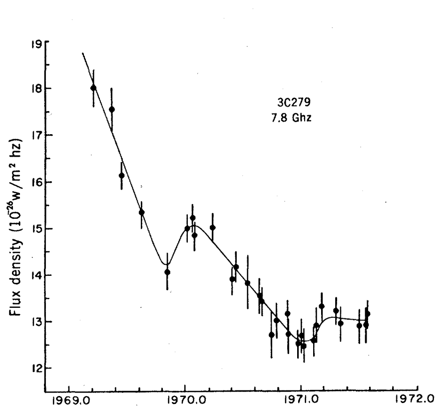

Fig. 1. The measured variations of the flux density of 3C279 at 7.8 Ghz.

It is the purpose of this report to present some measurements of the variations in the flux density of 3C279 at the same frequency as the interferometric observations and to show that these measurements are consistent with a model for 3C279 that does not involve an apparent expansion at superrelativistic speeds.

Figure 1 is a plot of the flux density of 3C279 measured at a frequency of 7.8 Ghz between 1969.0 and 1971.5 with a maser radiometer on the 120-foot Haystack antenna (1 foot = 0.3 m). These data were taken as part of an extensive program of monitoring variable sources that is being conducted at the Haystack Observatory (*4*). The errors associated with each flux density measurement have been conservatively estimated and can be considered to represent a 90 percent confidence limit.

It can be seen in Fig. 1 that the flux density of 3C279 has been generally decreasing since 1969.0 with a temporary minor increase in late 1969. This general decline is the remnant of a major radio outburst in 3C279 that began at this frequency in early 1966 (*5*). In 1965, before the outburst, the flux density was about 12 flux density units (10^{-26} watt m^{-2} hz^{-1}), and it can be seen from Fig. 1 that 3C279 again reached this minimum in early 1971.

The first set of VLBI observations (*1*) were made in mid-October 1970 (1970.79), when the flux density of 3C279 was 13.12 ± 0.05 units. This value was obtained from a least-squares linear curve fit to the measurements made between 1970.2 and 1971.0.

Between October 1970 and mid-February 1971, when the second set of VLBI observations were made, the flux density decreased to a minimum and then increased slightly to a value of 12.7 ± 0.10 units in mid-February (1971.13). The latter value was obtained from a fourth-order polynomial fit to the data taken after 1970.9. Thus, the total flux density of 3C279 had changed by 0.42 ± 0.12 unit over the same period that the fringe amplitude null was seen to move. Can the apparent null displacement have been caused by this observed change in flux density?

Since the fringe nulls are so deep, any source model must be very nearly symmetric during both interferometric observations. The simplest such model is one in which the source structure at 7.8 Ghz consists of an unresolved variable component situated midway between two static nonvarying components of equal amplitude (*6*). Figure 2 shows the computed location of the first fringe null in such a symmetric three-point-source model as a function of the ratio of the flux density of the central component to the sum of the flux densities of the two outer components (S_c/S_o). The computed null position is specified in terms of the corresponding projected interferometer spacing rela-

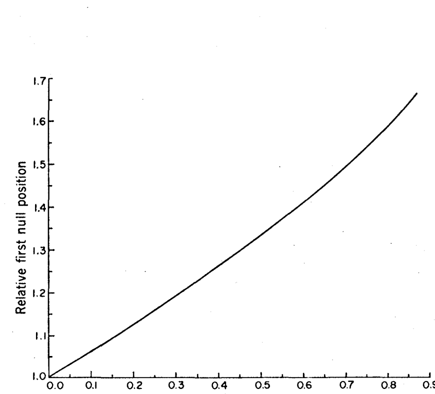

Fig. 2. The computed first null position as a function of the ratio of the flux density of the central component to the flux density of the two outer components (S_c/S_o) in the three-point-source model. The interferometer spacing (d) corresponding to the null has been normalized to the spacing (d_0) for which S_c would be 0.